TITLE

Extracellular vesicles derived from endometrial human mesenchymal stem cells enhance embryo yield and quality in an aged murine model

RUNNING TITLE

Vesicles from MSCs in aged blastocyst development

SUMMARY SENTENCE

The supplementation of embryo culture medium with extracellular vesicles from endometrial-derived mesenchymal stem cells increases the quality of aged embryos

KEYWORDS

Embryo culture, Stem cells, Proteomics, Gene expression, Oxidative stress, Aging

AUTHORS AND AFFILIATIONS

Federica Marinaro[1,‡], Beatriz Macías-García[3,‡,*], Francisco Miguel Sánchez-Margallo[1,2], Rebeca Blázquez[1,2], Verónica Álvarez[1], Elvira Matilla[3] , Nuria Hernández[3], María Gómez-Serrano[2,4] , Inmaculada Jorge[2,4], Jesús Vázquez[2,4], Lauro González-Fernández[5], Eva Pericuesta[6], Alfonso Gutiérrez-Adán[6], Javier G. Casado [1,2]

[1]Stem Cell Therapy Unit, Jesús Usón Minimally Invasive Surgery Centre (JUMISC), Cáceres, Spain.

[2]CIBER de Enfermedades Cardiovasculares (CIBERCV), Madrid, Spain.

[3]Assisted Reproduction Unit, Jesús Usón Minimally Invasive Surgery Centre, Cáceres, Spain.

[4]Centro Nacional de Investigaciones Cardiovasculares (CNIC), Madrid, Spain.

[5]Research Group of Intracellular Signaling and Technology of Reproduction (SINTREP), Institute of Biotechnology in Agriculture and Livestock (INBIO G+C), University of Extremadura, Cáceres, Spain

[6]INIA, Department of Animal Reproduction, Madrid, Spain.

CORRESPONDENCE

*Beatriz Macías García. Assisted Reproduction Unit, JUMISC.

N-521, Km 41.8, 10071, Cáceres. Email: bea_macias@hotmail.com.

ADDITIONAL FOOTNOTES.

‡Federica Marinaro and Beatriz Macías-García equally contributed to the present work and should be considered as co-first authors.

GRANT SUPPORT

This work was supported by one grant "Miguel Servet I" from Instituto de Salud Carlos III to JGC (CP17/00021 co-financed by FEDER/FSE); one grant Ramón y Cajal from the Spanish Ministry of Economy, Industry and Competitiveness (RYC-2017-21545; AEI/FEDER/UE) to BM-G; one grant MAFRESA S.L. to FM.

CONFERENCE PRESENTATIONS

Federica Marinaro, Eva Pericuesta, Francisco Miguel Sánchez-Margallo, Javier García Casado, Verónica Álvarez, Elvira Matilla, Nuria Hernández, Rebeca Blázquez, Lauro González-Fernández, Alfonso Gutiérrez-Adán and Beatriz Macías-García.The antioxidant activity of extracellular vesicles derived from endometrial human mesenchymal stem cells improves IVF outcome in an aged murine model. 22nd Annual ESDAR Conference 2018 Córdoba (Spain) September 27th-29th, 2018. Student oral competition.

ABSTRACT

Advanced age is a risk factor undermining women´s fertility. Hence, the optimization of assisted reproduction techniques is an interdisciplinary challenge that requires the improvement of *in vitro* culture systems. Here, we hypothesize that supplementation of embryo culture medium with extracellular vesicles from endometrial-derived mesenchymal stem cells (EV-endMSCs) may have a positive impact on the embryo competence of aged oocytes. In this work, 24 weeks old B6D2 female mice were used as egg donors and *in vitro* fertilization assays were performed using males from the same strain (8-12 weeks); the presumptive zygotes were incubated in the presence of 0, 10, 20, 40 or 80 µg/ml of EV-endMSCs. The results from the proteomic analysis of EV-endMSCs and the classification by reactome pathways allowed us to identify proteins closely related with the fertilization process. Moreover, in our aged murine model, the supplementation of the embryo culture medium with EV-endMSCs improved the developmental competence of the embryos as well as the total blastomere count. Finally, gene expression analysis of murine blastocysts showed significant changes on core genes related to cellular response to oxidative stress, metabolism, placentation and trophectoderm/inner cell mass formation. In summary, we demonstrate that EV-endMSCs increase the quality of the embryos, and according to proteomic and genomic analysis, presumably by modulating the expression of antioxidant enzymes and promoting pluripotent activity. Therefore, EV-endMSCs could be a valuable tool in human assisted reproduction improving the developmental competence of aged oocytes and increasing the odds of implantation and subsequent delivery.

INTRODUCTION

Advanced woman age is one of the most detrimental prognostic factors for fertility in humans as it decreases egg's competence. Nowadays, social, educational and financial pressures have delayed motherhood until the final thirties or forties, declining overall fertility and increasing the risk of miscarriage (1). When motherhood needs to be delayed, egg freezing is the assisted reproductive technique of choice to preserve the oocyte´s quality, but this has to be planned in advance which is not the most common scenario (2). In aged women (> 40 years), the use of assisted reproductive techniques is recommended if conception does not occur after 6 months. However, even when these techniques improve fertilization rates, blastocyst development is compromised and live births considerably decreased compared to oocytes´ from younger donors (3). This decline in fertility has been partly linked to an oxidative stress imbalance in the aged oocyte resulting in impaired reactive oxygen species metabolism and decreased capacity for protein/DNA repair (4). Nevertheless, the optimization of embryo culture conditions for aged oocytes is a challenge that could enhance embryo development and quality (5).

Nowadays, adult stem cells are under investigation to improve the fertilization rates in assisted reproduction. Placental derived mesenchymal stem cells (MSCs) are currently under evaluation in a clinical trial for improving implantation rates (Clinicaltrials.gov Identifier NCT01649752). Moreover, the therapeutic potential of autologous MSCs is evaluated in women suffering premature ovarian failure (Clinicaltrials.gov Identifier NCT02062931).

Special attention has been focused on the extracellular vesicles released by MSCs. They are known to mediate cell-to-cell communication by means of their specific cargo (RNAs, DNA, lipids, proteins, cytokines and growth factors) (6,7) and are secreted by different cell types including endometrial and oviductal cells (7–9). Furthermore, these extracellular vesicles have been used as coadjuvants in assisted reproduction (10). Their addition to bovine embryo culture medium has been found to enhance blastocyst quality (8,11) and to improve the

quality of homologous embryos through embryo-to-embryo communication when deriving derived from porcine parthenotes and bovine embryos (12,13).

Few years ago endometrial-derived Mesenchymal Stem Cells (endMSCs) and their extracellular vesicles (EV-endMSC) were isolated from menstrual blood (14) and they were found to alleviate human hepatic failure by diminishing active caspase 3 and apoptosis (15), to decrease prostate tumor-induced angiogenesis by modulating reactive oxygen species (ROS) production, diminishing VEGF secretion and NF-κB activity (16) and to exert cardioprotective effects through MicroRNA-21 (17). EV-endMSCs' importance in human reproduction has been demonstrated by the fact that they appeared to be involved in the embryo-maternal interactions (6) and in endometrial receptivity (18).

In view of these reports, and according to previous results from our group which demonstrated that human EV-endMSCs in embryo culture medium increased cell proliferation and hatching rates in a murine model (10), we hypothesize that human EV-endMSCs may have a beneficial effect on the developmental competence of embryos derived from aged females mice.

In order to validate this hypothesis, embryo division kinematics follow-up, blastocyst quality as well as the expression of specific genes were evaluated in zygotes derived from old mice (24 weeks old) after addition of EV-endMSCs. Additionally, the proteomic profile of the EV-endMSCs used for supplementation of embryo culture medium was characterized and classified using Gene Ontology and Reactome Pathway Database.

Materials and methods

Isolation and in vitro expansion of endometrial mesenchymal stromal/stem cells

Endometrial Mesenchymal Stromal/Stem Cells (endMSCs) were isolated from menstrual blood of four healthy women according to previously described protocols (10). Samples were

collected on day 2 or 3 of the menstrual cycle in a menstrual cup. Written informed consent was obtained from all donors under the auspices of the Minimally Invasive Surgery Centre Research Ethics Committee, which approved this study. Menstrual blood was diluted 1:2 in PBS and centrifuged at 450 x g for 10 min. Supernatants were discarded in order to remove cervical mucus debris and cells were re-suspended in Dulbecco's Modified Eagle's medium (DMEM) containing 10% fetal bovine serum (FBS), 1% penicillin/streptomycin and 1% glutamine. Cells were seeded onto tissue culture flasks and expanded at 37°C in 95% air and 5% CO_2 atmosphere. Non-adherent cells were removed after 24 hours. Adherent cells were cultured to 80% confluency and detached using PBS containing 0.25% trypsin (v/v). Cells were seeded again at a density of 5000 cells/cm^2. Culture medium was changed every three days.

Phenotypical characterization and multipotentiality of endMSCs

For the phenotypic analysis, 2×10^5 endMSCs were stained with human monoclonal antibodies (mAbs) against CD29, CD31, CD34, CD44, CD45, CD49d, CD49f, CD56, CD73, CD90, CD105 and HLA-DR using the appropriate concentrations of mAbs in the presence of PBS containing 2% FBS. The endMSCs and mAbs were incubated for 30 min at 4°C. Cells were then washed and re-suspended in PBS. Isotype-matched antibodies were used as negative controls. The flow cytometric analysis was performed on a FACScalibur cytometer (BD Biosciences, CA, USA) after acquisition of 10^5 events. Viable cells were selected using forward and side scatter characteristics and fluorescence was analyzed using CellQuest software (BD Biosciences, CA, USA). The mean relative fluorescence intensity (MRFI) was calculated by dividing the mean fluorescent intensity (MFI) by the MFI of its negative control. The differentiation assays of endMSCs were performed for 21 days with differentiation specific media, which was replaced every three days. Oil Red O, Alcian Blue and Alizarin Red S stainings were performed to evidence adipogenic, chondrogenic and osteogenic differentiation, respectively. Cells were analyzed at passages 3-4.

Isolation, purification and characterization of extracellular vesicles derived from endMSCs

Extracellular vesicles derived from endMSCs (EV-endMSCs) were obtained from endMSCs using a previously optimized protocol (10). The cell culture medium was DMEM (product code: L0102, Biowest, Nuaillé, France) containing 10% FBS) was replaced by DMEM containing 1% insulin–transferrin–selenium (product code: 41400045, ThermoFisher Scientific, Waltham, MA, USA) when cells reached 80% of confluence. End-MSCs at passages 4-5 were used for extracellular vesicles isolation. The endMSCs supernatants were collected every 3–4 days and centrifuged at 1000 x g for 10 min and 5000 x g for 20 min at 4°C. These supernatants were filtered using sterile cellulose acetate filters. Firstly, with a 0.45 µm pore size and secondly with a 0.2 µm pore size (Corning, NY, USA). Filtered supernatants were then concentrated using 3kDa MWCO Amicon® Ultra Devices (Merck-Millipore, MA, USA) centrifuged at 4000 x g for 1 hour at 4°C. The concentrated supernatants were stored at -20°C for the subsequent proteomic analysis and co-incubation with the zygotes.

Prior to *in vitro* experiments, the protein content of microvesicles was quantified by a Bradford assay (BioRad Laboratories, CA, USA). The concentration and size of purified extracellular vesicles were quantified by nanoparticle tracking analysis (NanoSight Ltd, Amesbury, UK) and analyzed using the particle-tracking analysis software package version 2.2.

Protein identification by high-resolution liquid chromatography coupled to mass spectrometry-based proteomic analyses

The characterization of EV-endMSCs from three different donors was performed by high-throughput proteomic analysis according to previously described protocols (19–23). For proteomic analysis, protein extracts were incubated with trypsin using the Filter Aides Sample Preparation (FASP) digestion kit (Expedeon), as previously described (24). The

resulting peptides were labelled using 8plex-iTRAQ reagents (Sciex) according to manufacturer´s instructions and desalted on OASIS HLB extraction cartridges (Waters Corp.). Half of the tagged peptides were directly analyzed by LC-MS/MS in different acquisition runs, and the remaining peptides were separated into 3 fractions using the high pH reversed-phase peptide fractionation kit (Thermo Fisher Scientific). High-resolution LC-MS analysis of iTRAQ-labelled peptides was carried out on an Easy nLC 1000 nano-HPLC apparatus (Thermo Scientific) coupled to QExactive mass spectrometer (Thermo Fisher Scientific). Peptides were injected onto a C18 reversed phase (RP) nano-column (75 µm I.D. and 50 cm, Acclaim PepMap100, Thermo Scientific) in buffer A (0.1% formic acid (v/v)) and eluted with a 180 min lineal gradient of buffer B (90% acetonitrile, 0.1% formic acid (v/v)). MS runs consisted of enhanced FT-resolution spectra (140,000 resolution) in the 390-1,500 m/z range and separated 390-700, 650-900, and 850-1500 m/z ranges followed by data-dependent MS/MS spectra of the 15 most intense parent ions acquired along the chromatographic run. HCD fragmentation was performed at 30% of normalized collision energy. A total of 14 MS data sets, eight from unfractionated material and six from the corresponding fractions, were registered with 42 hours total acquisition time. For peptide identification the MS/MS spectra were searched with the SEQUEST HT algorithm implemented in Proteome Discoverer 2.1 (Thermo Scientific). The results were analyzed using the probability ratio method (25) and the false discovery rate (FDR) of peptide identification was calculated based on the search results against a decoy database using the refined method (23). Peptide and scan counting was performed assuming as positive events those with a FDR equal or lower than 1%. Enrichment analysis was performed by using the DAVID functional annotation database (26,27). Abundance of proteins was estimated from LC/MS and quantified by means of the intensities of iTRAQ reporters. Reporter ion intensities were normalized to the total ion intensity of sample dataset.

Reagents

All the reagents were purchased from Sigma-Aldrich (Barcelona, Spain) unless otherwise stated.

Animals and superovulation protocol

All the experimental procedures were reviewed and approved by the Ethical Committee of the Junta de Extremadura (CGA/mbr). B6D2F1 mice were housed under a 12 hours light/12 hours dark cycle, at a controlled temperature (19-23°C) with free access to food and water. Females were intraperitoneally (IP) injected with 8 IU of equine chorionic gonadotropin (eCG, Veterin Corion, Divasa Farmavic) followed 49 hours later by 8 IU of IP human chorionic gonadotropin (hCG, Foligon, MSD) to trigger ovulation.

In Vitro Fertilization

Twenty four weeks old female mice (n = 24) were euthanized 12 hours after hCG administration by cervical dislocation, and cumulus-oocyte complexes (COCs) were recovered from oviducts and placed in 500 µl of pre-equilibtrated Human Tubal fluid (HTF; Merck-Millipore, Madrid, Spain) covered with mineral oil. Two male B6D2F1/J mice aged 8-12 weeks were euthanized (n = 16) for each IVF day by cervical dislocation and were ventrally dissected to remove the cauda epididymis. Once located, the epididymis and attached vas deferens were sectioned and transferred to two different a Petri dishes containing 500 µl of pre-equilibrated HTF covered with mineral oil. Spermatozoa were obtained by gently pressing the cauda epididymis through the vas deferens and were allowed to capacitate for 45 min at 37°C in a 5% CO_2/95% air atmosphere at 100% humidity. At the end of the incubation, sperm concentration was measured using a Makler chamber (Irvine Scientific, CA, USA). The pool of cumulus oocytes complexes obtained from all the females were released from the ampullas into a petri dish containing 500 µl of equilibrated HTF covered with mineral oil. Then, the oocytes were

inseminated with 2 × 10^6 sperm/ml pooled from both males (0.5 x 10^6 total sperm from each male); gametes were co-incubated for 6 hours, and the presumptive zygotes were washed in 500 µl ofclean KSOM medium after co-incubation (Merck-Millipore, Madrid, Spain). Then, zygotes were randomly allocated to 100 µl droplets of KSOM supplemented with 0, 10, 20, 40 or 80 µg/ml of EV-endMSCs and cultured until they reached the expanded blastocyst stage (4 days). Eight different IVF sessions in eight different days were run and 3 females (n=24) and 2 males (n=16) per day were used. Moreover, in order to show the differences between aged and non-aged oocytes in parallel with supplementation of EVs, we performed IVF on young B6D2 female mice (8-12 weeks, n=3). These IVF sessions were performed in accordance with the protocol used for the aged mice and no supplementation of EV-endMSCs was used.

Total cell number

The number of cells in an embryo is a well-known indicator of embryo quality (28). Therefore, to further evaluate embryo quality, some of the expanded blastocysts obtained were fixed in 4% formaldehyde in PBS added with 0.01% of polyvinyl alcohol (PVA; w/v) at 4˚C for 12 hours and stained with 2.5 µg/ml of Hoechst 33342 (Eugene, OR, USA) in PBS added with PVA for 10 minutes at 37˚C. Then, the blastocysts were mounted on glass slides with glycerol, covered with coverslips and sealed using nails polish. The embryos were then visualized using a fluorescence microscope (Nikon Eclipse TE2000-S) equipped with an ultraviolet lamp. Cell number was analyzed using the Fiji Image-J Software (1.45q, Wayne Rasband, NIH, USA).

RNA isolation and reverse transcription

Six independent samples of embryos cultured with and without EV-endMSCs (n = 25 expanded blastocysts per treatment) under each experimental condition (10 µg/ml, 20 µg/ml, 40 µg/ml, and 80 µg/ml of EV-endMSCs; n = 25 embryos/treatment) were used. Three independent groups of 8-9 embryos at blastocyst stage per experimental group were pooled and processed for poly(A) RNA extraction. Poly(A) RNA was extracted using the Dynabeads mRNA Direct

Extraction Kit (Dynal Biotech, Oslo, Norway) following the manufacturer's instructions with minor modifications as described by Bermejo-Alvarez and coworkers (29). After 5 min of incubation in lysis buffer and another 5 min with lysis buffer and Dynabeads, poly(A) RNA attached to the Dynabeads was extracted with a magnet and washed twice in washing buffer A and washing buffer B. RNA was then eluted with 10 mM Tris–HCl, pH 7.5. Immediately after extraction, the reverse transcription (RT) reaction was performed as recommended by the manufacturer (Epicentre Technologies Corp, Madison, WI, USA). Briefly, oligo-dT (0.2 µM) and random primers (0.5 µM) were added to each RNA sample and were heated for 5 min at 70°C to denature the secondary RNA structure. Next, the tubes were incubated at 25°C for 10 min to promote the annealing of the primers. Then, the RNA was reverse-transcribed for 60 min at 37°C in a final volume of 40 µL containing 0.375 mM dNTPs (Biotools, Madrid, Spain), 6.25 U RNasin RNAse inhibitor (Promega), 10 × MMLV-RT buffer with 8 mM dithiothreitol and 5 U MMLV high performance reverse transcriptase (Epicentre Technologies Corp, Madison, WI, USA), followed by incubation at 85°C for 5 min to inactivate the RT enzyme.

Gene expression analysis

The mRNA expression levels of the selected genes were determined by real-time quantitative reverse transcription polymerase chain reaction (qRT-PCR) using specific primers designed with Primer-BLAST (http://www.ncbi.nlm.nih.gov/ tools/primer-blast/) to span exon-exon boundaries when possible. Primers (Table 2) were previously validated for adequate primer efficiency; the specificity of their PCR products was confirmed by electrophoresis on a 2% agarose gel. All target genes showed efficiencies between 97 and 100% and correlation coefficients close to 1.0.

All PCR reactions were performed in a final volume of 20 µL, containing 0.25 mM of forward and reverse primers, 10 µL of GoTaq qPCR Master Mix (Promega) with SYBR Green as double-stranded DNA-specific fluorescent dye and 2 µL of each cDNA sample using a Rotorgene 6000

Real Time Cycler (Corbett Research, Sydney, Australia). For each experimental group, three different cDNA samples were used in two repetitions for all genes of interest. The PCR program consisted of an initial denaturalization step at 94°C for 2 min, followed by 35 cycles of denaturalization at 94°C for 10 s, annealing at 56°C for 30 s, extension at 72°C for 15 s and 10 s of fluorescence acquisition defined for each primer. At the end of each PCR run, melt curve analyses were performed for all genes to ensure single product amplification and exclude the possible interference of dimers.

Values were normalized using as housekeeping gene H2AFZ that were tested in previous studies (30). Relative expression levels were quantified by the comparative cycle threshold (ΔΔCT) method (31). Fluorescence was acquired in each cycle to determine the threshold cycle during the log-linear phase of the reaction at which fluorescence increased above background for each sample. According to the comparative CT method, the ΔCT value was determined by subtracting the mean CT value of the housekeeping gene for each sample from each gene CT value of the sample. Calculation of ΔΔCT involved using the highest sample ΔCT value (i.e. the sample with the lowest target expression) as an arbitrary constant to subtract from all other ΔCT sample values. Fold changes in the relative gene expression of the target were determined using the formula 2–ΔΔCT(32).

Internalization assay

To analyze the uptake of the EV-endMSCs by the embryos, the extracellular vesicles were stained with 2% SYTO RNA Select green fluorescent cell stain (Thermo Fisher Scientific) at 37°C for 30 min. PBS without exosomes were stained with 2% SYTO RNA Select green fluorescent cell stain and used as control. To remove the remaining dye, samples were centrifuged on exosome spin columns (MW 3000, Thermo Fisher Scientific) according to manufacturer's instructions. Exosomes concentration was indirectly measured in a Bradford assay. Finally, after IVF, 25 murine zygotes were co-cultured with labeled EV-endMSCs at different concentrations or stained PBS as negative control. Internalization (green fluorescence) was

confirmed by fluorescent microscopy. Additionally, embryos were stained with 2.5 mg/ml of Hoechst 33342 (Eugene, OR, USA) for 10 min at 37°C to visualize DNA.

Statistical analysis

For total cell number and gene expression analysis data were tested for normality using a Shapiro–Wilk test; results are reported as mean ± standard deviation (SD). Groups were compared using a one way ANOVA due their Gaussian distribution and homoscedasticity. When statistically significant differences were found, a Bonferroni post-hoc test was used to compare pairs of values in the blastomere count experiment, while for the expression of candidate genes, the ANOVA was followed by multiple pairwise comparisons using the Tukey method. Blastocyst rates were compared among groups by Chi-square test with the Yates correction for continuity. The Fisher's Exact Test was used when a value of less than 5 was expected in any treatment. Statistical analyses were performed using Sigma Plot software version 12.3 for Windows (Systat Software, IL, USA) or with SPSS-21 software (SPSS, IL, USA); $p < 0.05$ was considered as statistically significant.

Results

Characterization of endMSCs and EV-endMSCs

The characterization of endMSCs and EV-endMSCs has been previously published by our group (10,33). The phenotypical analysis evidenced that endMSCs were positive for CD29, CD44, CD73, CD90, CD105 and CD117, and negative for CD14, CD20, CD31, CD34, CD45, CD80 and HA-DR. The differentiation potential of these cells toward adipogenic, chondrogenic and osteogenic lineages was confirmed by selective staining and microscopic analysis after co-culture with differentiation specific media. Regarding EV-endMSCs, the nanoparticle tracking analysis showed that the mean size of the vesicles was 153.5±63.05 nm, while their

concentration was 3.31 x 10^{11}±3.8x10^{9} particles/ml. Additionally, the analysis of CD9 and CD63 by flow cytometry demonstrated a positive expression of these exosomal markers.

High-throughput proteomics analysis of EV-endMSCs

This proteomic analysis allowed us to identify a wide range of proteins in EV-endMSCs (n = 1802). The relative abundance of each protein, represented in Table 1, was estimated in accordance to the peptide counting from LC/MS analyses and was quantified by means of the intensities of iTRAQ reporters which were used to tag the peptides of each sample. Reporter ion intensities of each protein were normalized to the total ion intensity of the sample dataset. Functional analysis according to the Gene Ontology annotation database (34,35) was performed with the most representative proteins identified, accordingly to their abundance (n = 580), considering negligible proteins with abundance lower than 0.005%.

Firstly, the protein data set was classified according to the "cellular component" annotation. In this analysis, a total of 395 proteins were classified as *"Extracellular Vesicles"* (GO:1903561 $p < 0.01$, 5% FDR; data not shown). In a subsequent analysis using the Reactome Pathway Database (36) we sorted out the proteins according to their involvement in crucial pathways related to fertilization and embryo implantation. Some interesting Reactome pathways were: *Metabolism* (R-HSA-1430728; n = 114 proteins), *Developmental biology* (R-HSA-1266738; n = 74 proteins) and *Cellular response to oxidative stress* (R-HSA-2262752; n = 23 proteins). Figure 1 shows the Venn diagram with unique and overlapped proteins among these three Reactome pathways. Additionally, Table 1 lists the proteins identified and classified in the aforementioned Reactome categories. Of note, 45 out of 114 proteins identified in the *Metabolism pathway* were also classified by Gene-Ontology in the *Immune System Process* (GO:0002376). Similarly, 26 out of 114 were involved in the *Regulation of Cell Differentiation (*GO:0045595*).* Furthermore, the number of identified peptides (peptide counting) for each

protein together with the Gene name, UniProt Accession Code and the Reactome Pathway it belongs are listed in the Supplementary Table 1.

Development to the blastocyst stage and total cell number count

EV-endMSC addition to the embryo culture medium did not influence embryo division at days 1 and 2 of culture compared to control (Table 3; $p > 0.05$). However, when the embryos reached the morula stage (day 3), the 20 μg/ml and 80 μg/ml dosages of EV-endMSCs significantly enhanced the percentage of embryos that developed in culture compared to control (Table 3, $p < 0.05$). Our results showed that the blastocyst rate after 4 days of culture significantly increased when EV-endMSCs were added to the embryo culture medium at any of the dosages tested (Table 3; $p < 0.01$). Interestingly, the maximum blastocyst yield was observed for the 20 μg/ml dose (62.9% blastocyst rate) compared to the control (29.4%) at day 4 of culture.

In parallel, expanded blastocyst total cell number significantly increased for all the EV-endMSCs dosages tested varying from 32.4 ± 12.9 blastomeres per embryo (mean ± SD) in the control group to 48.5 ± 14.4 for the 40 μg/ml, being this the maximum value obtained (Figure 2; $p < 0.05$).

In order to emphasize the differences in developmental competence and kinematics of embryos obtained from young and aged female mice, new IVFs were performed in 8-12 week-old females in absence of EV-endMSCs. In our experimental conditions, the blastocyst rate in young females reached 89.6%, which was consistently higher than the percentages obtained in aged females (supplementary Table 2). To highlight the marked age-dependent differences found in IVF outcomes, a chi-square test was performed to compare the developmental competence and embryo kinematics of young (8-12 weeks) vs aged (24-26 weeks) B6D2 females. As it can be observed in the supplementary Table 2, blastocyst development was severely compromised with increasing age in our B6D2 females at all the stages studied.

Differential expression of embryo-related genes

The gene expression analysis was performed by quantitative PCR in blastocysts at day 4 of culture. Based on the proteomic analysis, several candidate genes were selected according to their involvement in the following Reactome categories: *Metabolism* (*Acaca, Gapdh*), *Cellular response to oxidative stress* (*Gpx1* and *Sod1*) and *Developmental biology* (*Pgf, Vegfa, Pou5f1* and *Sox2*). These four genes were also subclassified according to their involvement in placentation (*Pgf*, *Vegfa*) and trophectoderm/inner cell mass formation (*Pou5f1* and *Sox2*). When compared against control, the relative RNA abundance for *Gpx1* was downregulated in the 20-80 µg/ml EV-endMSCs while *Sod1* expression was consistently lower in the 10-40 µg/ml doses ($p < 0.05$). Relative *Vegfa* and *Gapdh* expression increased at all the EV-endMSCs doses used compared to control ($p < 0.05$) except for the 80 µg/ml dose which did not differ from the non-EV-endMSCs added treatment ($p > 0.05$). *Sox2* expression was upregulated for the 10, 20 and 40 µg/ml dosage compared to control ($p < 0.05$), while its expression did not change when EV-endMSC at 80 µg/ml were added ($p > 0.05$; Figure 3).

In addition, the relative RNA abundance of *Acaca, Pgf and Pouf51* did not vary despite EV-endMSC supplementation ($p > 0.05$; Figure 3).

EV-endMSCs uptake

Fluorescent labelling of EV-endMSCs allowed us to confirm that these vesicles are effectively internalized by the embryos after 24 h of co-culture. The absence of fluorescence in the control demonstrated that residual fluorescence was not interfering with analysis. Based on the fluorescence analysis, here we demonstrated that EV-endMSCs co-cultured with murine embryos at different concentrations were rapidly internalized. Figure 4 shows representative images of a murine embryo co-cultured with EV-endMSCs at 80 µg/ml, as well as representative images of the control.

Discussion

In the present study, we demonstrate that extracellular vesicles released from human endometrial MSCs can be used as an embryo culture supplement to partially recover the developmental competence of aged oocytes. In our setting, not only the developmental competence of the embryos was improved (Table 3), but also the total blastomere count (Figure 2). This is in accordance with the report of Qu et al., who demonstrated that bovine embryos subjected to somatic cell nuclear transfer produce exosomes that enhance the development to the blastocyst stage as well as their quality (13).

Even when embryo culture conditions have lesser influence on the developmental potential of the early embryo than the initial oocyte quality (37), our results in an aged murine model demonstrate that EV-endMSCs enhance the developmental competence as well as the quality of the embryos produced. These results may have discrepancies with former reports in mice and bovine where addition of extracellular vesicles did not enhance the embryo's developmental competence (8,10,11). However, it is important to note that, in our previous report (10), these EV-endMSCs were co-cultured with 2-cell embryos retrieved from young females (aged 8-12 weeks) which have a notably superior developmental competence than the aged murine model used in the present work. This consideration can also be confirmed by our results regarding the developmental competences of zygotes retrieved from young and aged females (Supplementary Table 2). As expected, in absence of the EVs supplementation, embryos from young female mice were significantly more capable of developing when compared to the embryos from aged females. This result demonstrates that improving the developmental competence of embryos derived from young B6D2 females is virtually not possible. On the contrary, it is possible to improve embryo development in aged murine models. So naturally ageing mice can be considered important models for the investigation of occurring declines in reproductive capacity and impaired viability of the oocyte (38).

In the case of the bovine species (8,11), embryo culture medium was enriched with homologous oviductal extracellular vesicles and the reduced developmental competence of *in vitro* matured oocytes could not be overcome when these vesicles were used. This divergence can be explained not only by the molecular differences that may exist between human EV-endMSCs and bovine oviductal extracellular vesicles, but also by the inherent reduced developmental competence of bovine oocytes harvested in prophase I (39).

On the other hand, mesenchymal stem cells have been previously used for embryo culture in porcine, bovine and murine models; even when contradictory results have been reported, it has been proposed that MSCs secrete growth factors that may have a positive impact during embryo culture enhancing embryo quality (40–42).

Next, in order to further understand the mechanisms involved in the beneficial effects of EV-MCs on the embryo development, a high throughput proteomic analysis was performed in these EV-endMSCs. Firstly, the most abundant identified proteins were classified according to specific Reactome pathways which are closely related with the fertilization process: *Metabolism* (a total of 114 proteins), *Developmental biology* (a total of 74 proteins) and *Cellular response to oxidative stress* (a total of 23 proteins; Table 1).

Some of the most abundant proteins found in our proteomic analysis deserve better investigation. For example, fibronectin (FN1) was reported to be essential for embryogenesis, from the two-cell stage to tissue morphogenesis (43–46). Vinculin (VCL) and Alpha2 macroglobulin (A2M), other abundant proteins found in our analysis, were found to be important during early development (47,48). Moreover, A2M as well as Matrix metalloproteinase-3 (MMP-3) and Agrin (AGRN) were related to implantation (49–51). In addition, Matrix metalloproteinase -2 (MMP-2) and Laminin beta 1 (LAMB1) were associated to the developing human embryo and the early phases of human pregnancy (52,53).

Interestingly, the proteomic analysis revealed the presence of four different Insulin-like growth factor-binding proteins isoforms (-4, -5, -6, -7) in all EV-endMSCs samples. The presence of

these proteins is relevant considering that previous reports have demonstrated that the addition of insulin-like growth factor-binding protein to embryo culture medium protects the inner cell mass from apoptosis and increases mitochondrial membrane potential in oocytes (54). Our proteomic analysis has also demonstrated a very high abundance of serum albumin (the fourth in terms of absolute quantification), which is largely used for the supplementation of commercial media in IVF (55) and has been reported to alleviate ROS production *in vitro* in neurons and sperm (56,57).

To further confirm if the proteomic results can, at least in part, explain the improvement in the developmental competence and embryo quality, gene expression analysis in the resulting blastocysts was performed on core genes related to *Cellular response to oxidative stress, Metabolism, Placentation and Trophectoderm/inner cell mass formation.*

Regarding the *cellular response to oxidative stress* category, previous studies have evidenced that one of the main constraints blunting the developmental competence of aged oocytes relies on their reduced ability to counteract ROS (58). Interestingly, the expression of *Sod1* (as well as *Gpx1)* consistently decreased at the 20 and 40 µg/ml EV-endMSCs dosages coinciding with the highest embryo yields obtained in the present work (Figure 3 and Table 3). The diminished expression of glutathione peroxidase 1 and superoxide dismutase 1 suggests that EV-endMSCs exert an exogenous ROS scavenger activity during embryo culture (Figure 3). As a matter of fact, a good correlation between mRNA, proteins and antioxidant enzyme activities in embryos subjected to diabetic environment has already been demonstrated (59). In the pre-implantation embryo, antioxidant enzymes (including SOD1 and GPX1) are primarily regulated at the pre-transcriptional level, and the transcripts are translated to produce active enzymes (60). Moreover, it was postulated that embryo's defense against ROS depends the intracellular ROS levels that trigger the expression of antioxidant genes as demonstrated in human umbilical vein endothelial cells (61)and mouse zygotes (62). It has to be noted that, in our work, EV-endMSCs were added to zygotes. In view of all the previous literature and

considering that major gene activation occurs in the 2-cell embryo, if less *Sod1* and *Gpx1*mRNA is found in the embryos, it is likely that lower ROS levels are triggering their expression. Agreeing with our findings, but in the setting of prostate tumors, EV-endMSCs have also been shown to diminish angiogenesis in tumoral cells by means of their ROS scavenger activity (16), demonstrating again the ROS scavenger potential of EV-endMSCs is an unexplored scenario. Additionally, the expression levels of *Pou5f1* and *Sox2* were also analyzed. The gene *Pou5f1* is a homeodomain transcription factor of the POU (Pit-Oct-Unc), family that encodes the Oct4 protein. This protein has been shown to be a critical regulator of cellular pluripotency in murine embryos (63). Additionally, the transcription factor Sox2 (SRY-related HMG-box gene 2) forms a complex with Oct4 and participates in the maintenance of self-renewal of the pluripotent inner cell mass, being essential for the formation of the trophoectoderm in the preimplantation embryo (64). Our results demonstrate that the expression of *Pou5f1* did not vary between treatments but the expression of *Sox2* raised for the 10-40 µg/ml EV-endMSCs dosages coinciding with the maximum blastocyst rates and total cell number (Figure 3). It is known that morulae developed from *Sox2-/-* zygotes get arrested at this stage and fail to cavitate (64) and form a proper inner cell mass (65); in addition, rescue experiments using cell-permeant Sox2 protein result in increased blastocyst rate and restoration of Sox2 protein levels in murine blastocysts knock-down of *Sox2* using short interfering RNA (64). Hence, the increased expression of *Sox2* together with the enhanced developmental competence and cell number of our embryos further corroborate the boosting effect on embryo quality mediated by EV-MSCs supplementation.

Regarding to metabolism-related genes, it has been demonstrated that fully pluripotent stem lines exhibit higher ATP levels compared with initial pluripotent stem cells (66). These observations are coincident with the increased *Gapdh* expression and increased total cell number observed in our embryos for the 10-40 µg/ml EV-endMSCs dosages. It is widely known that GAPDH activity is involved in the glycolytic pathway triggering the conversion of

glyceraldehyde-3-phosphate to 1,3-diphosphoglycerate to provide energy in the form of ATP. Hence, the increased expression of *Sox2* in our aged murine model suggests that firstly, EV-endMSCs increases the quality of the embryos through the self-renewal of the pluripotent inner cell mass and the establishment of the trophectoderm lineage (64). Secondly, the increased expression of *Gapdh* suggests an increase of embryo quality through the enhancement of metabolism during embryonic development.

Conversely, our results did not show significant differences in the expression levels of the *Acaca* gene which encodes the acetyl-CoA carboxylase, suggesting that fatty acid metabolism is not affected by EV-endMSCs supplementation to the embryo culture medium.

Aside from quality-related genes and metabolism-related genes, we aimed to determine if the produced embryos could potentially exhibit higher implantation ability. Our experiments revealed that *Vegfa* consistently increased when EV-endMSCs were added at the 10-40 µg/ml dosages. Previous reports have demonstrated that mouse-derived embryos treated with either recombinant human VEGF, or VEGF isoforms 121 and 165, exhibit higher embryo development with quicker cavitation, increased blastomere number, improved implantation rates and fetal limb development compared to controls (67). Furthermore, recent findings from our research group have demonstrated that murine embryos exposed to EV-endMSCs exhibit higher VEGF and PDGF-AA release, confirming the results of the present study (8). Therefore, the addition of EV-endMSCs to IVF-derived murine zygotes obtained from aged females increased the quality of the embryos, presumably due to their ROS scavenger and pluripotent-promoting activity. Furthermore, in light of the previously mentioned reports it is tempting to speculate that the resulting embryos may also exhibit higher implantation potential.

To the authors' best knowledge, this is the first report describing the proteomic profiling of EV-endMSCs based on Reactome pathways. Moreover, our *in vitro* assays have demonstrated their therapeutic potential to rescue the developmental competence of aged oocytes in a murine model. Hence, their beneficial effect should be taken in account as it may be a valuable

tool in human ARTs improving the efficiency of the current techniques and increasing the odds of implantation and subsequent delivery.

FUNDING

This work was supported in part by CIBER-CV (CB16/11/00494, CB16/11/00277). Two projects from Junta de Extremadura (IB16168 co-financed by FEDER/FSE). One grant "Miguel Servet I" from Instituto de Salud Carlos III to JGC (CP17/00021 co-financed by FEDER/FSE), one grant Ramón y Cajal from the Spanish Ministry of Science, Innovation and Universities (RYC-2017-21545; AEI/FEDER/UE) to BM-G; one grant MAFRESA S.L. to FM.

The competitive projects from the Ministry of Science, Innovation and Universities (AGL2015-73249-JIN, AGL2015-66145, AGL2017-84681-R (AEI/FEDER/UE), and the Carlos III Institute of Health-Fondo de Investigación Sanitaria (PRB2, PT13/0001/0017-ISCIII-SGEFI/FEDER; PBR3, PT17/0019/0003 ISCIII-SGEFI/FEDER; ProteoRed), and the Fundación La Marato TV3 (20153731(122/C/2015). The CNIC is supported by the Ministry of Science, Innovation and Universities and the Pro CNIC Foundation, and is a Severo Ochoa Center of Excellence (SEV-2015-0505). All i*n vitro* studies were performed at the ICTS Nanbiosis (Units 14, 22 and 23). The funders had no role in study designs, data collection and analysis, decision to publish or preparation of the manuscript.

ACKNOWLEDGEMENTS

The authors wish to acknowledge the generous donation of the menstrual blood. In addition, the work from the animal housing staff Luis Dávila, Marisa Higuero and Víctor Pérez who exquisitely took care of the animals used in this study is greatly appreciated.

COMPETING INTERESTS

The authors have declared that no competing interests exist.

BIBLIOGRAPHY

1. Rasool S, Shah D. The futile case of the aging ovary: is it mission impossible? A focused review. Climacteric. 2018 Jan 2;21(1):22–8.

2. Allahbadia GN. Social Egg Freezing: Developing Countries Are Not Exempt. J Obstet Gynecol India. 2016 Aug;66(4):213–7.

3. O'Brien YM, Ryan M, Martyn F, Wingfield MB. A retrospective study of the effect of increasing age on success rates of assisted reproductive technology. Int J Gynecol Obstet. 2017 Jul;138(1):42–6.

4. Mihalas BP, Redgrove KA, McLaughlin EA, Nixon B. Molecular Mechanisms Responsible for Increased Vulnerability of the Ageing Oocyte to Oxidative Damage. Oxid Med Cell Longev. 2017;2017:1–22.

5. Highet AR, Bianco-Miotto T, Pringle KG, Peura A, Bent S, Zhang J, et al. A novel embryo culture media supplement that improves pregnancy rates in mice. Reproduction. 2017 Mar;153(3):327–40.

6. Greening DW, Nguyen HPT, Elgass K, Simpson RJ, Salamonsen LA. Human Endometrial Exosomes Contain Hormone-Specific Cargo Modulating Trophoblast Adhesive Capacity: Insights into Endometrial-Embryo Interactions1. Biol Reprod [Internet]. 2016 Feb 1 [cited 2017 Nov 28];94(2). Available from: https://academic.oup.com/biolreprod/article-lookup/doi/10.1095/biolreprod.115.134890

7. Théry C, Zitvogel L, Amigorena S. Exosomes: composition, biogenesis and function. Nat Rev Immunol. 2002;2(8):569–79.

8. Lopera-Vasquez R, Hamdi M, Maillo V, Gutierrez-Adan A, Bermejo-Alvarez P, Ramírez MÁ, et al. Effect of bovine oviductal extracellular vesicles on embryo development and quality *in vitro*. Reproduction. 2017 Apr;153(4):461–70.

9. Wang L, Yu Z, Wan S, Wu F, Chen W, Zhang B, et al. Exosomes Derived from Dendritic Cells Treated with Schistosoma japonicum Soluble Egg Antigen Attenuate DSS-Induced Colitis. Front Pharmacol. 2017;8:651.

10. Blázquez R, Sánchez-Margallo FM, Álvarez V, Matilla E, Hernández N, Marinaro F, et al. Murine embryos exposed to human endometrial MSCs-derived extracellular vesicles exhibit higher VEGF/PDGF AA release, increased blastomere count and hatching rates. Afink GB, editor. PLOS ONE. 2018 Apr 23;13(4):e0196080.

11. Lopera-Vásquez R, Hamdi M, Fernandez-Fuertes B, Maillo V, Beltrán-Breña P, Calle A, et al. Extracellular Vesicles from BOEC in In Vitro Embryo Development and Quality. Sturmey R, editor. PLOS ONE. 2016 Feb 4;11(2):e0148083.

12. Saadeldin IM, Kim SJ, Choi YB, Lee BC. Improvement of Cloned Embryos Development by Co-Culturing with Parthenotes: A Possible Role of Exosomes/Microvesicles for Embryos Paracrine Communication. Cell Reprogramming. 2014 Jun;16(3):223–34.

13. Qu P, Qing S, Liu R, Qin H, Wang W, Qiao F, et al. Effects of embryo-derived exosomes on the development of bovine cloned embryos. PloS One. 2017;12(3):e0174535.

14. Khoury M, Alcayaga-Miranda F, Illanes SE, Figueroa FE. The promising potential of menstrual stem cells for antenatal diagnosis and cell therapy. Front Immunol. 2014;5:205.

15. Chen L, Xiang B, Wang X, Xiang C. Exosomes derived from human menstrual blood-derived stem cells alleviate fulminant hepatic failure. Stem Cell Res Ther [Internet]. 2017 Dec [cited 2018 Mar 2];8(1). Available from: http://stemcellres.biomedcentral.com/articles/10.1186/s13287-016-0453-6

16. Alcayaga-Miranda F, González PL, Lopez-Verrilli A, Varas-Godoy M, Aguila-Díaz C, Contreras L, et al. Prostate tumor-induced angiogenesis is blocked by exosomes derived from menstrual stem cells through the inhibition of reactive oxygen species. Oncotarget [Internet]. 2016 Jul 12 [cited 2018 Mar 2];7(28). Available from: http://www.oncotarget.com/fulltext/9852

17. Wang K, Jiang Z, Webster KA, Chen J, Hu H, Zhou Y, et al. Enhanced Cardioprotection by Human Endometrium Mesenchymal Stem Cells Driven by Exosomal MicroRNA-21: Superiority of Endometrium Mesenchymal Stem Cells. STEM CELLS Transl Med. 2017 Jan;6(1):209–22.

18. Homer H, Rice GE, Salomon C. Review: Embryo- and endometrium-derived exosomes and their potential role in assisted reproductive treatments-liquid biopsies for endometrial receptivity. Placenta. 2017 Jun;54:89–94.

19. Bonzon-Kulichenko E, Pérez-Hernández D, Núñez E, Martínez-Acedo P, Navarro P, Trevisan-Herraz M, et al. A robust method for quantitative high-throughput analysis of proteomes by 18O labeling. Mol Cell Proteomics MCP. 2011;10(1):M110.003335.

20. García-Marqués F, Trevisan-Herraz M, Martínez-Martínez S, Camafeita E, Jorge I, Lopez JA, et al. A Novel Systems-Biology Algorithm for the Analysis of Coordinated Protein Responses Using Quantitative Proteomics. Mol Cell Proteomics MCP. 2016;15(5):1740–60.

21. Jorge I, Navarro P, Martínez-Acedo P, Núñez E, Serrano H, Alfranca A, et al. Statistical model to analyze quantitative proteomics data obtained by 18O/16O labeling and linear ion trap mass spectrometry: application to the study of vascular endothelial growth factor-induced angiogenesis in endothelial cells. Mol Cell Proteomics MCP. 2009 May;8(5):1130–49.

22. Navarro P, Trevisan-Herraz M, Bonzon-Kulichenko E, Núñez E, Martínez-Acedo P, Pérez-Hernández D, et al. General statistical framework for quantitative proteomics by stable isotope labeling. J Proteome Res. 2014 Mar 7;13(3):1234–47.

23. Navarro P, Vázquez J. A refined method to calculate false discovery rates for peptide identification using decoy databases. J Proteome Res. 2009;8(4):1792–6.

24. Wiśniewski JR, Ostasiewicz P, Mann M. High recovery FASP applied to the proteomic analysis of microdissected formalin fixed paraffin embedded cancer tissues retrieves known colon cancer markers. J Proteome Res. 2011 Jul 1;10(7):3040–9.

25. Martínez-Bartolomé S, Navarro P, Martín-Maroto F, López-Ferrer D, Ramos-Fernández A, Villar M, et al. Properties of average score distributions of SEQUEST: the probability ratio method. Mol Cell Proteomics MCP. 2008 Jun;7(6):1135–45.

26. Huang DW, Sherman BT, Lempicki RA. Systematic and integrative analysis of large gene lists using DAVID bioinformatics resources. Nat Protoc. 2009;4(1):44–57.

27. Huang DW, Sherman BT, Lempicki RA. Bioinformatics enrichment tools: paths toward the comprehensive functional analysis of large gene lists. Nucleic Acids Res. 2009 Jan;37(1):1–13.

28. Alpha Scientist in Reproductive Medicine and ESHRE Special Interest Group of Embryology. The Istanbul consensus workshop on embryo assessment: proceedings of an expert meeting. Hum Reprod. 2011 Jun 1;26(6):1270–83.

29. Bermejo-Álvarez P, Rizos D, Rath D, Lonergan P, Gutierrez-Adan A. Epigenetic differences between male and female bovine blastocysts produced in vitro. Physiol Genomics. 2008 Jan;32(2):264–72.

30. Bermejo-Alvarez P, Rizos D, Rath D, Lonergan P, Gutierrez-Adan A. Sex determines the expression level of one third of the actively expressed genes in bovine blastocysts. Proc Natl Acad Sci. 2010 Feb 23;107(8):3394–9.

31. Schmittgen TD, Livak KJ. Analyzing real-time PCR data by the comparative C(T) method. Nat Protoc. 2008;3(6):1101–8.

32. Livak KJ, Schmittgen TD. Analysis of Relative Gene Expression Data Using Real-Time Quantitative PCR and the 2−ΔΔCT Method. Methods. 2001 Dec;25(4):402–8.

33. Álvarez V, Sánchez-Margallo FM, Macías-García B, Gómez-Serrano M, Jorge I, Vázquez J, et al. The immunomodulatory activity of extracellular vesicles derived from endometrial mesenchymal stem cells on CD4+ T cells is partially mediated by TGFbeta. J Tissue Eng Regen Med. 2018 Oct;12(10):2088–98.

34. Ashburner M, Ball CA, Blake JA, Botstein D, Butler H, Cherry JM, et al. Gene ontology: tool for the unification of biology. The Gene Ontology Consortium. Nat Genet. 2000;25(1):25–9.

35. The Gene Ontology Consortium. Expansion of the Gene Ontology knowledgebase and resources. Nucleic Acids Res. 2017 Jan 4;45(D1):D331–8.

36. Fabregat A, Jupe S, Matthews L, Sidiropoulos K, Gillespie M, Garapati P, et al. The Reactome Pathway Knowledgebase. Nucleic Acids Res. 2018 Jan 4;46(D1):D649–55.

37. Lonergan P, Fair T. Maturation of Oocytes in Vitro. Annu Rev Anim Biosci. 2016;4:255–68.

38. Thouas GA, Trounson AO, Jones GM. Effect of female age on mouse oocyte developmental competence following mitochondrial injury. Biol Reprod. 2005 Aug;73(2):366–73.

39. Lonergan P, Fair T. In vitro-produced bovine embryos—Dealing with the warts. Theriogenology. 2008 Jan;69(1):17–22.

40. Bhardwaj R, Ansari MM, Parmar MS, Chandra V, Sharma GT. Stem Cell Conditioned Media Contains Important Growth Factors and Improves In Vitro Buffalo Embryo Production. Anim Biotechnol. 2016;27(2):118–25.

41. Opiela J, Bülbül B, Romanek J. Varied Approach of Using MSCs for Bovine Embryo In Vitro Culture. Anim Biotechnol. 2018 Apr 30;1–8.

42. Park H-Y, Kim E-Y, Lee S-E, Choi H-Y, Moon JJ, Park M-J, et al. Effect of human adipose tissue-derived mesenchymal-stem-cell bioactive materials on porcine embryo development. Mol Reprod Dev. 2013 Dec;80(12):1035–47.

43. de Almeida PG, Pinheiro GG, Nunes AM, Gonçalves AB, Thorsteinsdóttir S. Fibronectin assembly during early embryo development: A versatile communication system between cells and tissues. Dev Dyn Off Publ Am Assoc Anat. 2016 Apr;245(4):520–35.

44. Larson RC, Ignotz GG, Currie WB. Effect of fibronectin on early embryo development in cows. J Reprod Fertil. 1992 Sep;96(1):289–97.

45. Raddatz E, Monnet-Tschudi F, Verdan C, Kucera P. Fibronectin distribution in the chick embryo during formation of the blastula. Anat Embryol (Berl). 1991;183(1):57–65.

46. Tsuiki A, Preyer J, Hung TT. Effects of fibronectin and its peptide fragment on preimplantation mouse embryo. Am J Obstet Gynecol. 1989 Mar;160(3):724–8.

47. Duband JL, Thiery JP. Spatio-temporal distribution of the adherens junction-associated molecules vinculin and talin in the early avian embryo. Cell Differ Dev Off J Int Soc Dev Biol. 1990 Apr;30(1):55–76.

48. Hong S-K, Dawid IB. Alpha2 macroglobulin-like is essential for liver development in zebrafish. PloS One. 2008;3(11):e3736.

49. Coppock HA, White A, Aplin JD, Westwood M. Matrix metalloprotease-3 and -9 proteolyze insulin-like growth factor-binding protein-1. Biol Reprod. 2004 Aug;71(2):438–43.

50. Bauersachs S, Mitko K, Ulbrich SE, Blum H, Wolf E. Transcriptome studies of bovine endometrium reveal molecular profiles characteristic for specific stages of estrous cycle and early pregnancy. Exp Clin Endocrinol Diabetes Off J Ger Soc Endocrinol Ger Diabetes Assoc. 2008 Jul;116(7):371–84.

51. Esadeg S, He H, Pijnenborg R, Van Leuven F, Croy BA. Alpha-2 macroglobulin controls trophoblast positioning in mouse implantation sites. Placenta. 2003 Nov;24(10):912–21.

52. Pereza N, Ostojić S, Volk M, Kapović M, Peterlin B. Matrix metalloproteinases 1, 2, 3 and 9 functional single-nucleotide polymorphisms in idiopathic recurrent spontaneous abortion. Reprod Biomed Online. 2012 May;24(5):567–75.

53. Roediger M, Miosge N, Gersdorff N. Tissue distribution of the laminin beta1 and beta2 chain during embryonic and fetal human development. J Mol Histol. 2010 Apr;41(2–3):177–84.

54. Ascari IJ, Alves NG, Jasmin J, Lima RR, Quintão CCR, Oberlender G, et al. Addition of insulin-like growth factor I to the maturation medium of bovine oocytes subjected to heat shock: effects on the production of reactive oxygen species, mitochondrial activity and oocyte competence. Domest Anim Endocrinol. 2017;60:50–60.

55. Blake D, Svalander P, Jin M, Silversand C, Hamberger L. Protein Supplementation of Human IVF Culture Media. J Assist Reprod Genet. 2002 Mar;19(3):137–43.

56. Macias-Garcia B, Gonzalez-Fernandez L, Loux SC, Rocha AM, Guimaraes T, Pena FJ, et al. Effect of calcium, bicarbonate, and albumin on capacitation-related events in equine sperm. Reproduction. 2014 Nov 28;149(1):87–99.

57. Vega L, Arroyo ÁA, Tabernero A, Medina JM. Albumin-Blunted Deleterious Effect of Amyloid-β by Preventing the Internalization of the Peptide into Neurons. J Alzheimers Dis. 2009 Jul 23;17(4):795–805.

58. Tatone C, Amicarelli F, Carbone MC, Monteleone P, Caserta D, Marci R, et al. Cellular and molecular aspects of ovarian follicle ageing. Hum Reprod Update. 2008 Apr;14(2):131–42.

59. Forsberg H, Borg LA, Cagliero E, Eriksson UJ. Altered levels of scavenging enzymes in embryos subjected to a diabetic environment. Free Radic Res. 1996 Jun;24(6):451–9.

60. Guérin P, El Mouatassim S, Ménézo Y. Oxidative stress and protection against reactive oxygen species in the pre-implantation embryo and its surroundings. Hum Reprod Update. 2001 Apr;7(2):175–89.

61. Maître B, Jornot L, Junod AF. Effects of inhibition of catalase and superoxide dismutase activity on antioxidant enzyme mRNA levels. Am J Physiol. 1993 Dec;265(6 Pt 1):L636-643.

62. Schultz RM. Regulation of zygotic gene activation in the mouse. BioEssays News Rev Mol Cell Dev Biol. 1993 Aug;15(8):531–8.

63. Wu G, Schöler HR. Role of Oct4 in the early embryo development. Cell Regen. 2014;3(1):3:7.

64. Keramari M, Razavi J, Ingman KA, Patsch C, Edenhofer F, Ward CM, et al. Sox2 Is Essential for Formation of Trophectoderm in the Preimplantation Embryo. Pera M, editor. PLoS ONE. 2010 Nov 12;5(11):e13952.

65. Rizzino A, Wuebben EL. Sox2/Oct4: A delicately balanced partnership in pluripotent stem cells and embryogenesis. Biochim Biophys Acta BBA - Gene Regul Mech. 2016 Jun;1859(6):780–91.

66. Zhang Y, Cui P, Li Y, Feng G, Tong M, Guo L, et al. Mitochondrially produced ATP affects stem cell pluripotency *via* Actl6a-mediated histone acetylation. FASEB J. 2018 Apr;32(4):1891–902.

67. Binder NK, Evans J, Gardner DK, Salamonsen LA, Hannan NJ. Endometrial signals improve embryo outcome: functional role of vascular endothelial growth factor isoforms on embryo development and implantation in mice. Hum Reprod. 2014 Oct 10;29(10):2278–86.

FIGURE LEGENDS

Figure 1. High-throughput proteomic analysis on EV-endMSCs. Protein extracts from EV-endMSCs were processed by high-resolution liquid chromatography coupled to mass spectrometry-based proteomic analyses. The functional enrichment analysis was performed by Reactome Pathway Database in the most representative proteins identified (n = 580). The Venn diagram shows unique and overlapped proteins in these three Reactome pathways.

Figure 2. Total cell number of murine blastocysts cultured in presence or absence of EV-endMSCs. Total cell number of the expanded blastocysts was obtained after Hoechst 33342 staining and subsequent evaluation by fluorescence microscopy. For each treatment, the individual blastomere count is represented. Horizontal bars show the mean values. All the treatments differ statistically from the control ($p < 0.05$).

Figure 3. Relative mRNA expression of candidate genes. Relative mRNA levels of candidate genes related to the proteome categories cellular response to oxidative stress, metabolism and developmental biology (n = 25 embryos/treatment). Bars represent mean ± SD; values bearing different letters differ statistically from the control ($p < 0.05$).

Figure 4. Internalization of EV-endMSCs by the embryos. EV-endMSCs were labeled with SYTO RNA Select green fluorescent cell stain and co-cultured at different concentrations with embryos for 24 h. Additionally, embryos were stained with Hoechst to visualize DNA. The figure shows representative images of an embryo co-cultured with EV-endMSCs at 80 µg/ml (E, F, G, H). Representative images of the control (embryos co-cultured with stained PBS) are also shown (A, B, C, D). A and E: bright field microscopy showing a representative embryo. B and F: visualization of Hoechst fluorescence under fluorescence microscopy. C and G: visualization of SYTO RNA Select fluorescence under fluorescence microscopy. D: merged image of A, B and C. H: merged image of E, F and G.

TABLES

Table 1. Reactome functional annotation of EV-endMSCs proteins. Proteins were classified and subsequently analyzed according to their involvement in crucial pathways related to in vitro fertilization and embryo implantation. Selected pathways were Metabolism (R-HSA-1430728) (n=114 identified proteins), Developmental biology (R-HSA-1266738) (n=74) and Cellular response to oxidative stress (R-HSA-2262752) (n=23). Color scale represents the protein abundance according to total peptide counting from LC/MS analyses. Additional information regarding LC/MS protein identification is displayed in Supplementary Table 1.

Table 2. List of primers.

Table 3. Embryo division kinematics and blastocyst rate. Murine oocytes from aged females (24 weeks old) were subjected to IVF and the number of oocytes used as well as their embryo division dynamics was recorded at days 1 to 4 of embryo culture. All values are presented as

total number and (percentage); values bearing different letters in the same column differ statistically from the control ($p < 0.05$).

Supplementary Table 1. Proteins identified in EV-endMSCs LC/MS analyses at 1% FDR (n=1802). Protein descriptions, UniProt accession codes and the corresponding genes names (N/A means "Not assigned") are displayed. **Np** refers to the number of peptides identified for each protein. The FDR for peptide identification was set at 1%. Green symbols indicate those proteins annotated within the Reactome pathways discussed on the text (Table 1).

Figure 1

Click here to download Figure Figura 1.tif

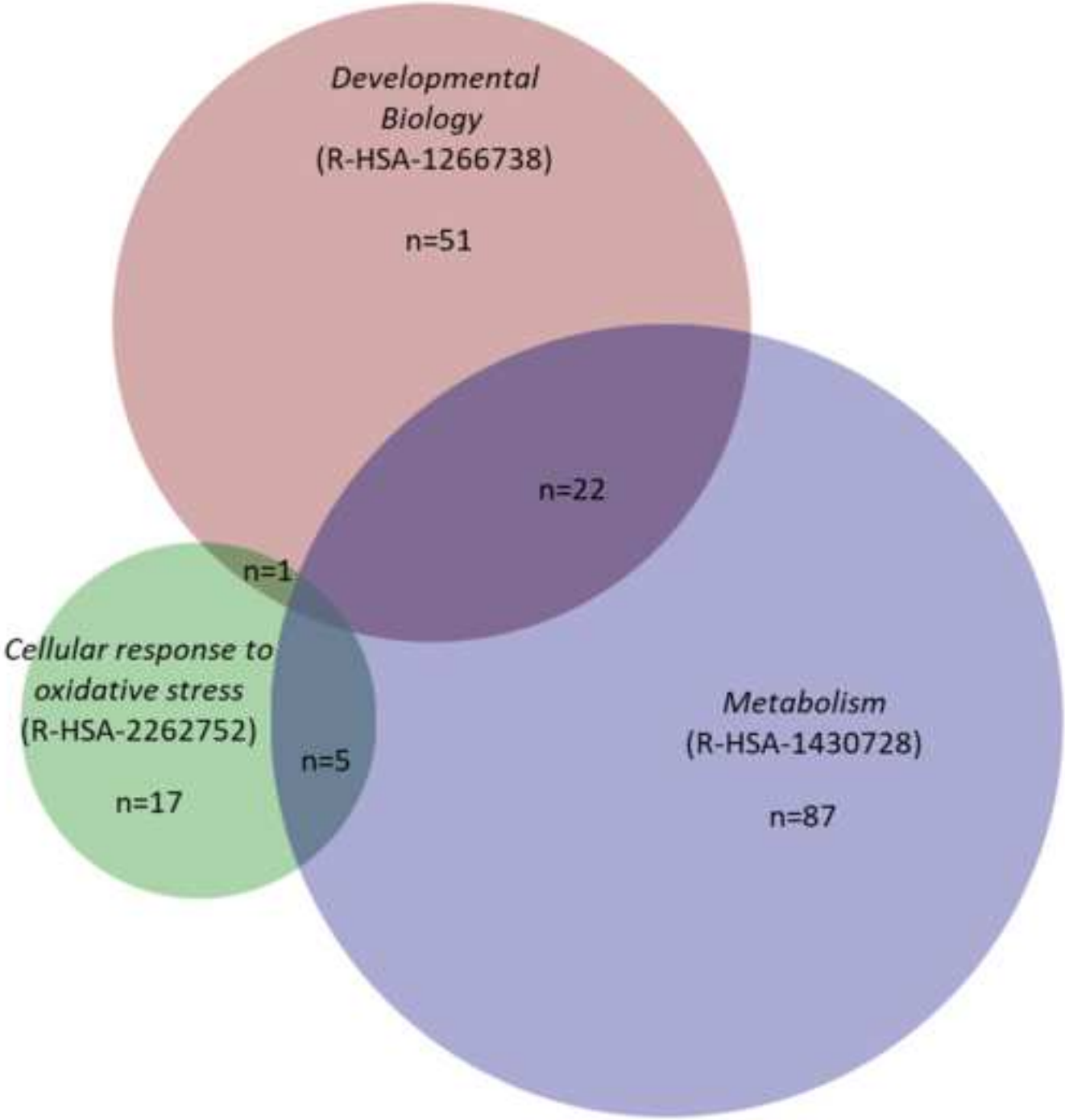

Figure 2

Click here to download Figure Figure 3.jpg

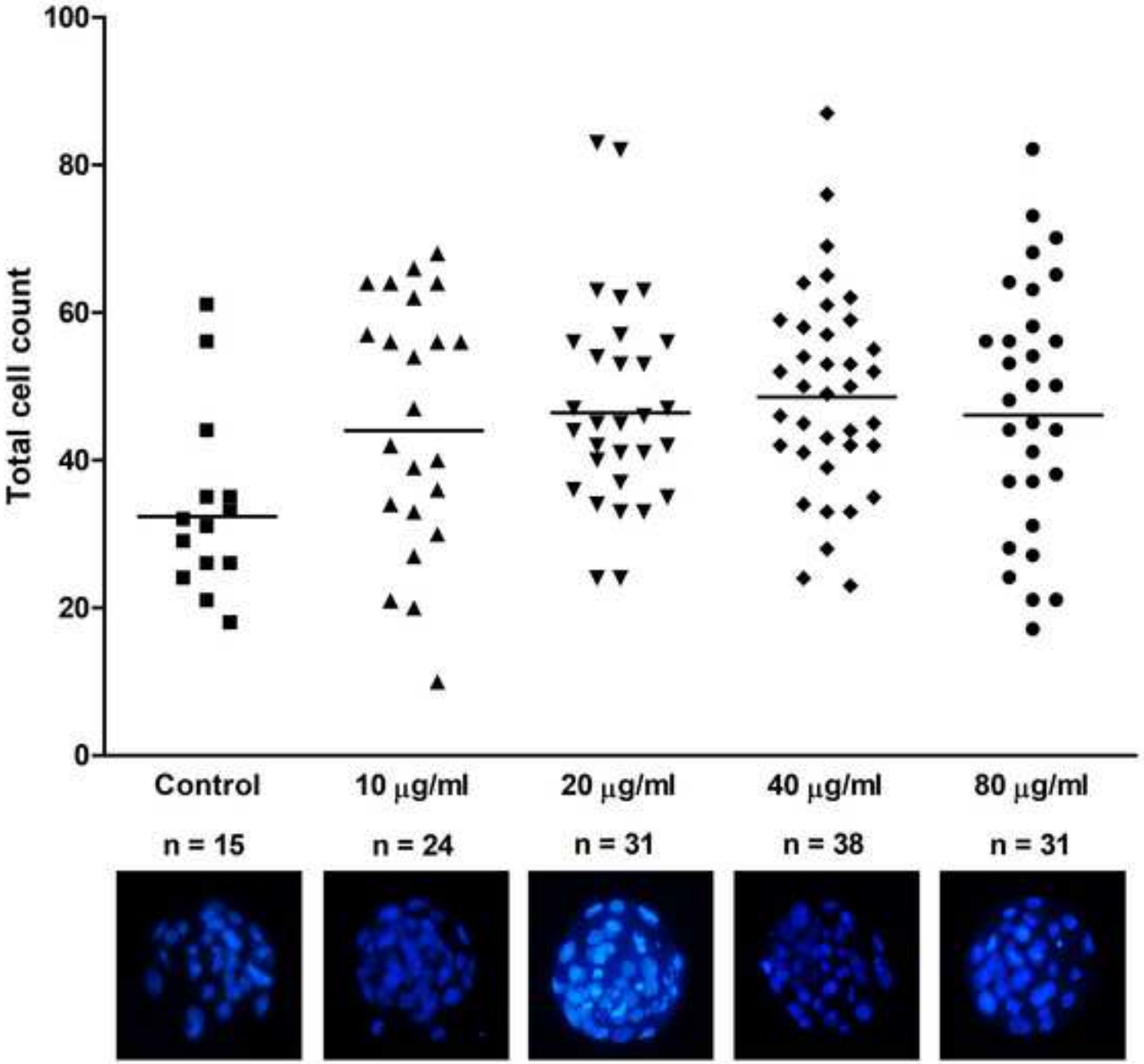

Figure 3

Click here to download Figure Figure 2.jpg

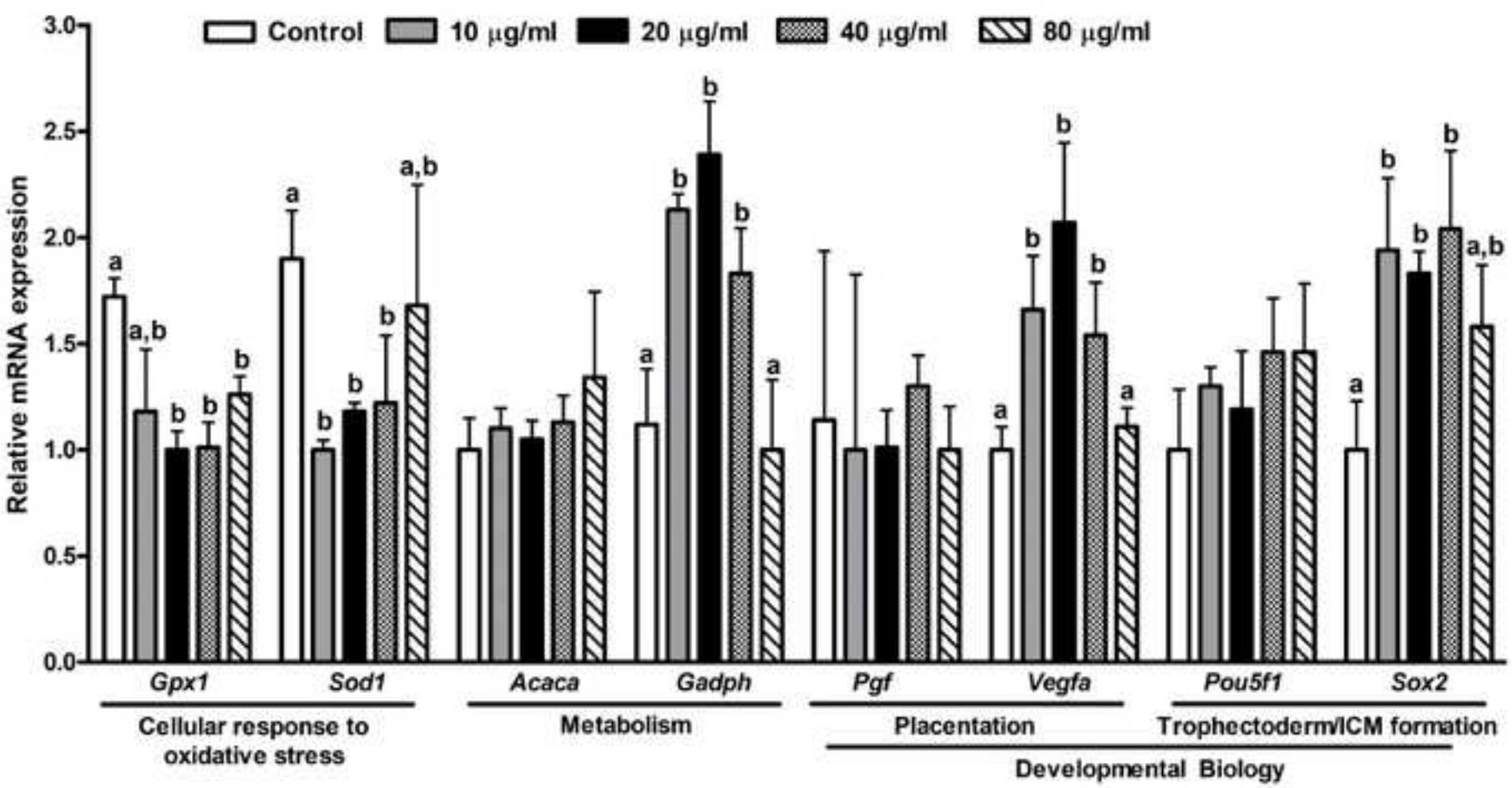

Table 1.

Metabolism		Developmental Biology		Cellular response to oxidative stress
PSMA3	A2M	ACTR2	PSME2	SOD2
GM2A	PSMB4	ARPC2	PRNP	MMP3
PSAP	NME2	PSMA3	PSMA6	SOD1
GSS	KPNB1	PEA15	CFL1	SOD3
CNDP2	TKT	MYL12A	GPC1	HSPA1B
GOT2	ATP5B	IQGAP1	ACTN2	PARK7
LDHA	ENO1	HSP90AB1	SDC2	PRDX2
IQGAP1	FDPS	COL5A1	CDH2	ANXA1
PSMA1	MANBA	PFN1	MYH14	PRDX1
FABP5	MAN2B2	PSMA1	MMP2	APEX1
PGK1	ALDOC	ALCAM	ACTR3	PDGFD
IDH1	GSTP1	CAP1	LAMB1	TXNRD1
GLO1	TXN	PLXNC1	SPTAN1	PDGFRA
FH	ADH5	NEO1	HSPA8	PTPRK
SDC4	ME1	PSMB3	COL3A1	TPM1
PSMB3	ALB	FN1	VCL	GSTP1
HSPG2	PGAM2	AGRN	PSMB7	TXN
BTD	PSMA5	PEBP1	LAMC1	CYCS
LTA4H	HK1	PDGFRB	HSP90AA1	AXL
RPLP2	B4GAT1	PSME1	COL6A1	CST3
TPI1	LRP1	COL6A3	DPYSL2	PRDX5
AGRN	PSMA4	FABP4	PDGFRA	PRDX6
HBB	CYCS	UBA52	PSMB1	P4HB
PSAT1	AP2B1	MSN	SEMA3A	
PSME1	PRSS1	MYL9	EZR	
NAGLU	PGD	PSMA7	PSMB4	
MARCKS	PSME2	MYH10	TLN1	
DCN	SEC23A	ITGB1	SEMA7A	
HEXB	MDH2	PDLIM7	COL6A2	
FABP4	PSMA6	MYH11	YWHAB	
UBA52	ALDH1A1	PSMB9	NRP1	
PSMA7	GPC1	COL5A2	ACTB	
PGK2	PGAM1	MYH9	COL2A1	
GC	LUM	PSMA2	ARPC4	
PTGDS	EXT1	PSMA4	PSMA5	
HEXA	GALNS	AP2B1	MYL6	
RBP1	EXT2	TUBA1B	SPTBN1	
CTGF	TALDO1			
GNS	GBE1			
GLRX	ALDOA			
PSMB9	PGLS			
ENO3	SDC2			
APOE	DBI			
RPL12	DDAH2			
VCAN	GAPDH			
PSMA2	RPLP1			
CMPK1	CD44			
LDHB	P4HB			
TXNRD1	CBR1			
NT5E	MDH1			
APOA1	CKM			
RPS28	PCSK9			
PSMB1	PSMB7			
GSTO1	ACP5			
SDC1	GPI			
TCN2	BGN			
NME1	HSP90AA1			

Table 2.

Entrez gene symbol	Gene name	Accesion no.	Forward primer (5'-3')	Reverse primer (5'-3')	Product length
H2afz	H2A histone family, member Z	NM_001316995.1	AGGACGACTAGCCATGGACGTGTG	CCACCACCAGCAATTGTAGCCTTG	209
Gpx1	Glutathiones peroxidase 1	NM_001329527.1	GCAACCAGTTTGGGCATCA	CTCGCACTTTTCGAAGAGCATA	116
Pgf	Placental Growth Factor	NM_001271705.1	CTCTCTGGAACACAGGCAGA	CCGTAGCTGTACCACGAAGA	100
Vegfa	Vascular endothelial growth factor A	NM_009505	CACAGCAGATGTGAATGCAG	TTTACACGTCTGCGGATCTTG	94
Acaca	acetyl-Coenzyme A carboxylase alpha	XM_011248666.1	AAACCAGCACTCCCGATTCAT	GGCCAAACCATCCTGTAAGC	175
Pou5f1	POU domain, class 5, transcription factor 1	NM_013633	TAGGTGAGCCGTCTTTCCAC	GCTTAGCCAGGTTCGAGGAT	159
Sox2	SRY (sex determining region Y)-box 2	NM_011443.4	GCACATGAACGGCTGGAGCAACG	TGCTGCGAGTAGGACATGCTGTAGG	206
Bax	BCL2-associated X protein	NM_007527.3	AAGCTGAGCGAGTGTCTCCGGCG	GCCACAAAGATGGTCACTGTCTGCC	361
Gapdh	Glyceraldehyde-3-Phosphate Dehydrogenase	NM_001289726.1	AGGTCGGTGTGAACGGATTTG	TGTAGACCATGTAGTTGAGGTCA	122
Sod1	Superoxide Dismutase 1	NM_174615	GTGCAAGGCACCATCCACTTCG	CACCATCGTGCGGCCAATGATG	309
Gadd45a	Growth Arrest And DNA Damage Inducible Alpha	BC023815.1	CTTCTGGTCGCACGGGAAGG	GCTCCACCGCGGCAGTCACC	277

Table 3. Embryo division kinematics.

	Oocytes	**2 cells (Day 1)**	**8 cells (Day 2)**	**Morula (Day 3)**	**Blastocyst (Day 4)**
Control	126	93 (73.8)	82 (65.1)	71(56.3)[a]	37 (29.4)[a]
10 µg/ml	124	98 (79)	95 (76.6)	83 (66.9)[a]	56 (45.2)[b]
20 µg/ml	124	102 (82.3)	96(77.4)	95 (76.6)[b]	78 (62.9)[b]
40 µg/ml	128	97 (75.8)	88 (68.8)	86 (67.2)[a]	71 (55.5)[b]
80 µg/ml	130	104 (80)	100 (76.9)	93 (71.5)[b]	70 (53.8)[b]